



Soft tissue absorption tomography with correction for scattering aberrations.

Emilie Franceschini, Marie-Christine Pauzin, Serge Mensah, Jean-Philippe Groby

► To cite this version:

Emilie Franceschini, Marie-Christine Pauzin, Serge Mensah, Jean-Philippe Groby. Soft tissue absorption tomography with correction for scattering aberrations.. Ultrasonic Imaging, 2005, 27, pp.221-236. hal-00086833

HAL Id: hal-00086833

<https://hal.science/hal-00086833>

Submitted on 18 Dec 2008

HAL is a multi-disciplinary open access archive for the deposit and dissemination of scientific research documents, whether they are published or not. The documents may come from teaching and research institutions in France or abroad, or from public or private research centers.

L'archive ouverte pluridisciplinaire **HAL**, est destinée au dépôt et à la diffusion de documents scientifiques de niveau recherche, publiés ou non, émanant des établissements d'enseignement et de recherche français ou étrangers, des laboratoires publics ou privés.

Soft tissue Absorption Tomography with Correction for Scattering Aberrations *

EMILIE FRANCESCHINI¹, MARIE-CHRISTINE PAUZIN¹,
SERGE MENSAH¹, JEAN-PHILIPPE GROBY²

¹Laboratoire de Mécanique et d'Acoustique - CNRS
31 Chemin Joseph Aiguier,
13402 Marseille Cedex 20 - France

²Laboratory of Acoustics and Thermal Physics,
Celestijnenlaan 200D, B-3001 Heverlee - Belgium

Abstract

Among the many factors involved in ultrasound attenuation phenomena, scattering effects play a major role, even in the unexpected case of soft tissues. It is proposed in this study to quantitatively evaluate the scattering affecting the measurements, before reconstructing the absorption parameter alone.

The reconstruction procedure involves three steps: i/ estimating the sound speed map using a transmission tomography algorithm. This estimation procedure provides a numerical phantom of the organ probed, cleared of all dissipative components. This absorption free phantom mimics the (viscoacoustic) tissues imaged except for the density and absorption characteristics: the density a priori equals 1000 kg/m³, and the absorption is not taken into account. The impedance fluctuations in the object are therefore approximated on the basis of the sound speed contrast; ii/ synthesizing the field scattered by the absorption free phantom; the attenuation observed here results solely from the scattering phenomenon. The synthesis is carried out using a finite-element time domain code simulating the ultrasonic propagation through the phantom. It provides the scattering distortion reference introduced into the log spectral absorption estimator; iii/ reducing the scattering distortions affecting the integrated absorption measured along the ray paths using a log spectral procedure.

The corrected integrated absorption is then processed using a tomographic reconstruction procedure that provides an estimate of the absorption distribution. Simple numerical simulations show the improvement obtained in the absorption estimates with this approach.

KEY WORDS: Absorption tomography; scattering; viscoacoustic propagation model; ultrasound.

*Version without annexes of the preprint submitted to Ultrasonic Imaging

1 Introduction

During the past four decades, many clinical studies have suggested that a diagnostic imaging device sensitive to differences in the attenuation of tissues would be useful for improving detection and characterization procedures [1]-[5].

Several methods have been proposed for estimating ultrasound attenuation, which can be roughly subdivided into time domain [6]-[9] and frequency domain methods [10]-[14]. Although time-based techniques are generally easier to use than spectral techniques when making real time measurements, most authors have adopted a spectral approach [15]. Since tissue attenuation and beam diffraction are both frequency dependent, estimates obtained in the frequency domain tend to be more accurate and the results more consistent. Unfortunately, in vivo tissue attenuation measurements are difficult to perform [15]: ultrasound attenuation estimates are generally affected by many factors. Some of these factors, such as phase cancellation, transducer bandwidth, beam diffraction and focusing, which are system dependent, have been addressed using dedicated correction techniques [16]-[20]. Another important process, which is often underestimated as far as soft tissues are concerned, is the scattering induced by inhomogeneities [21]-[23], which is one of the two main attenuation mechanisms at work in tissues, the other being the absorption by the medium due to dissipative processes. When dealing with inhomogeneous media, it is obviously rather difficult to separate the contributions of these two mechanisms. This is why the scattering has received little attention so far in the case of soft tissues, since the sound speed variations usually amount to less than 10%.

In absorption transmission tomography studies, two simplifying assumptions are generally made. First, the diffraction¹ effects are ignored; this is equivalent to assuming that wave phenomena can be accounted for in terms of ray acoustics. The second assumption is that the propagation is rectilinear and that no refraction therefore occurs. Based on these hypotheses, the absorption images produced [25] are often spoiled by artefacts. Several research groups have attempted to correct the refraction effects using iterative techniques based on numerical ray tracing methods [26] or an alternative approach using a perturbation analysis of refraction [27]. However, when the size of the inhomogeneities present in the object are of the same order of magnitude as the wavelength, the ray theory approach is no longer reliable.

The aim of the present study is to provide means of accounting for the scattering effects from which standard absorption tomographic techniques suffer. The error introduced by the scattering in the log spectral difference method is evaluated and a scattering correction technique is proposed. Absorption reconstructions based on simulated data show the improvement obtained using this method.

2 Scattering effects in ultrasound absorption estimation

In order to describe the scattering effects induced by the inhomogeneities present in the medium, we assume that the ultrasound device is a linear system and, within the narrow bandwidth usually used in ultrasound methods, that the tissue absorption increases linearly with the frequency [28] $\alpha(\mathbf{x}, f) = \alpha_0(\mathbf{x})f$. f is the frequency in Hz; $\alpha(\mathbf{x}, f)$ is the frequency dependent absorption coefficient of the tissue at any point \mathbf{x} on a cross-sectional plane. $\alpha_0(\mathbf{x})$ is the absorption

¹Diffraction corresponds here to wave processes that cannot be accounted for in terms of ray acoustics. On the other hand, scattering refers to all reflection processes, whether specular or not [24].

coefficient of linear frequency dependence (in $\text{Np} \cdot \text{cm}^{-1} \cdot \text{MHz}^{-1}$). A similar analysis of the scattering effects on the insertion log spectral difference technique has been proposed by Xu and Kaufman [21], who took into consideration the transducer diffraction induced distortion. Here it is proposed to focus on the scattering due to the heterogeneities present in the medium.

Let us consider two transducers, one transmitter and one receiver placed in a water tank and make two measurements: one with and one without the tissue placed between the transducers. The amplitude spectrum $Y_w(f)$ of the ultrasound signal propagating through the water (reference signal) equals:

$$|Y_w(f)| = |Y_0(f)H_w(f)| \quad (1)$$

where $Y_w(f)$ is the Fourier transform of the recorded signal $y_w(t)$ defined by $Y_w(f) = \int_{-\infty}^{\infty} y_w(t)e^{-i2\pi ft} dt$.

$Y_0(f)$ is the spectral instrumental function, which includes the amplitude spectrum of the electrical input signal and the transfer functions of the transmitting and receiving transducers. $H_w(f)$ characterizes the effects of the scattering on the ultrasound pulse along the water path alone, corresponding to the transducer diffraction.

The amplitude spectrum $Y_{mes}(f)$ of the signal recorded with the tissue inserted corresponds to:

$$|Y_{mes}(f)| = |Y_0(f)H_w(f)H_{sc}(f)| e^{-\int_{ray} \alpha_0(\mathbf{x}) ds} f \quad (2)$$

where $H_{sc}(f)$ characterizes the effects of the scattering processes on the ultrasound pulse along the water - tissue - water propagation path.

Log spectral difference technique

The linear model described above is generally written in the case of a homogeneous layer of tissue probed by a plane wave so that the interfaces encountered are perpendicular to the beam; only absorption occurs in this case. The integrated absorption $A_w(f)$ is the slope of the log spectral ratio $|Y_w(f)/Y_{mes}(f)|$ versus the frequency f [10]:

$$A_w(f) = \int_{ray} \alpha_{0w}(\mathbf{x}) ds = \frac{\ln |Y_w(f)| - \ln |Y_{mes}(f)|}{f} \quad (3)$$

where α_{0w} is the absorption coefficient estimated when the scattering effects are neglected. This technique is no longer relevant when ultrasonic absorption tomography is performed on complex tissue structures where the interfaces are not necessarily perpendicular to the beam. The lack of scattering considerations will inevitably result in large errors in the estimated absorption coefficient. Instead of using Eq.(3), the integrated absorption coefficient $A(f)$ is derived from Eq.(2):

$$A(f) = \int_{ray} \alpha_0(\mathbf{x}) ds = \frac{\ln |Y_w(f)| - \ln |Y_{mes}(f)| + \ln |H_{sc}(f)|}{f} \quad (4)$$

The error introduced when Eq.(3) is used instead of Eq.(8) is the scattering induced distortion $D(f)$:

$$D(f) = \int_{ray} (\alpha_0(\mathbf{x}) - \alpha_{0w}(\mathbf{x})) ds = \frac{\ln |H_{sc}(f)|}{f} \quad (5)$$

3 Correction of scattering effects

It is now proposed to separate the scattering and dissipative mechanisms that contribute to the attenuation phenomenon by estimating $D(f)$ and then calculating $A(f) = A_w(f) + D(f)$.

For this purpose, we will attempt to predict the field scattered by the organ. In the first step, in order to obtain a rough approximation of the scattering processes, we reconstruct the velocity map of the object investigated. This velocity map is associated with a constant density map (1000 kg/m^3) and a null attenuation map in order to build up a dissipation free acoustical model that we have named the *numerical phantom* or simply the *phantom*. We simulate ultrasonic wave propagation through this phantom using a finite element time domain propagation code. The amplitude spectrum $Y_{sim}(f)$ of the pulse recorded after the simulated wave propagation through the phantom (inserted between the two transducers) is given by:

$$|Y_{sim}(f)| = |Y_0(f)H_w(f)\widetilde{H_{sc}}(f)| \quad (6)$$

where $\widetilde{H_{sc}}(f)$ characterizes the effects of the scattering on the ultrasound pulse along the water - phantom - water propagation path. Similar spectra are obtained in the absence of the phantom (water reference $Y_w(f)$). The scattering induced distortion $\widetilde{D}(f)$ is then estimated by:

$$\widetilde{D}(f) = \frac{\ln |\widetilde{H_{sc}}(f)|}{f} = \frac{\ln |Y_{sim}(f)| - \ln |Y_w(f)|}{f} \quad (7)$$

and is removed from the water-reference integrated absorption $A_w(f)$ in order to obtain the estimated integrated absorption $\widetilde{A}(f)$:

$$\widetilde{A}(f) = \int_{ray} \widetilde{\alpha}_0(\mathbf{x}) ds = \frac{\ln |Y_{sim}(f)| - \ln |Y_{mes}(f)|}{f} \quad (8)$$

The (estimated) integrated absorption $\widetilde{A}(f)$ is therefore given by the slope of the log spectral ratio $|Y_{sim}(f)/Y_{mes}(f)|$ versus the frequency f . Lastly, a transmission tomographic procedure is used to determine the estimated absorption distribution $\widetilde{\alpha}_0(\mathbf{x})$.

For this correction method to work, the scattering effects have to be fairly similar in both the tissue sample and the numerical phantom so that the relation $H_{sc}(f) \approx \widetilde{H_{sc}}(f)$ is acceptable. The sound speed, density and absorption fluctuations all contribute to the scattering effects. In practice, the density map is not known and in order to overcome the fact that the parameter distributions are difficult to observe, we assume that the object has a constant density equal to 1000 kg/m^3 . In the case of adipose tissues, this will be an overestimate, and in that of muscle and stroma tissues, it will be an underestimate. The impedance fluctuations are therefore approximated by the sound speed variations.

4 Application to simulated data

In order to assess the scattering correction procedure, we consider a numerical tissue-like model (Fig. 1) whose scattering response is computed using a Finite Element time domain Method (FEM). This method has been extended to include absorption-dispersion effects. The governing numerical expressions on which the FEM is based can be found in the references [29] and [30].

A grid consisting of 1730×1730 pixels ($\Delta x = 0.016$ mm, 27.7 mm \times 27.7 mm) is used. The ring antenna, which is composed of 360 equally spaced transducers (point-like transmitters and receivers, central frequency 2.5 MHz, $\lambda = 0.6$ mm), has a radius of $R = 13.2$ mm. Each transducer emits a short pulse, while the remaining elements act as receivers. The temporal and spectral plots of the transmitted pulses are shown in figure 2. The academic cylindrical model, which is immersed in water (density 1000 kg/m³, velocity 1500 m/s), simulates a fluid object having the following characteristics: density 950 kg/m³, velocity 1470 m/s (without any dissipative considerations) and absorption 6 Np/m/MHz. The external radius of the cylinder is 11 mm. The diameters of the inclusions are $d_0 = 8\lambda = 3.6$ mm, $d_1 = 4\lambda = 2.4$ mm and $d_2 = 2\lambda = 1.2$ mm. The inclusions have the following characteristics: density 1060 kg/m³, velocity 1600 m/s (without any dissipative considerations) and absorption 19 Np/m/MHz. Figure 3 shows the variations $\alpha(f)/f$ in function of f obtained with the viscoacoustic code. One can observe here that the simulated absorption $\alpha(f)$ is almost linear with the frequency in the case of both tissues.

Figure 4 illustrates the velocity map reconstructed using the layer stripping technique presented in the references [31] [32]. The average estimate of the inclusion sound speed is 1634 m/s and the standard deviation is 15%, which corresponds to the dispersion curves given in figure 5. In the case of the inclusions, the dispersion (Fig. 5) induces sound speed changes in the 20 m/s to 30 m/s range in the 1.5 - 4 MHz frequency bandwidth.

Ultrasound propagation was simulated through the estimated absorption free phantom having the velocity map shown in figure 4 and the scattering correction procedure was applied. We must point out that we have regularized the inclusions borders (the inclusions were given the shape of regular ellipses) in order to prevent irregularities in shape from increasing the scattering phenomenon. Tomographic reconstructions were performed using the fan beam algorithm described by Kak and Slaney [33]. 360 projections taken over an angle of 360° in transmission were used. In figure 6, in the case of a given transmitter ($x = 0.65$ mm, $y = 13.85$ mm), the projection data of the analytical integrated absorption and the estimated integrated absorption (obtained with the simulated data) are compared. At receivers 90° to 270° (those used in transmission tomography), the absorption estimates were greatly improved, especially in the case of the two largest inclusions 8λ and 4λ in diameter. In the case of these two inclusions, the maximum relative error was 53% without correcting and 7% after correcting the scattering effects.

Figures 7 and 8 show the reconstructions obtained when the integrated absorption was calculated neglecting the scattering effects, as in Eq.(3), after correcting the scattering effects, as done in Eq.(8), respectively. In the case of the classical reconstruction method (Fig. 7), one can note the artefacts (concentric circles) around the two biggest inclusions. Figure 9 gives the corresponding line profiles of both reconstructions. Both reconstructions with and without correction of the scattering effects show that with both methods, objects of twice the wavelength can be detected. Scattering correction makes it possible to discriminate the size and to evaluate the absorption of objects of four times the wavelength (Fig. 8). In the case of the smallest inclusions, neither of these methods of reconstruction was satisfactory, however. The

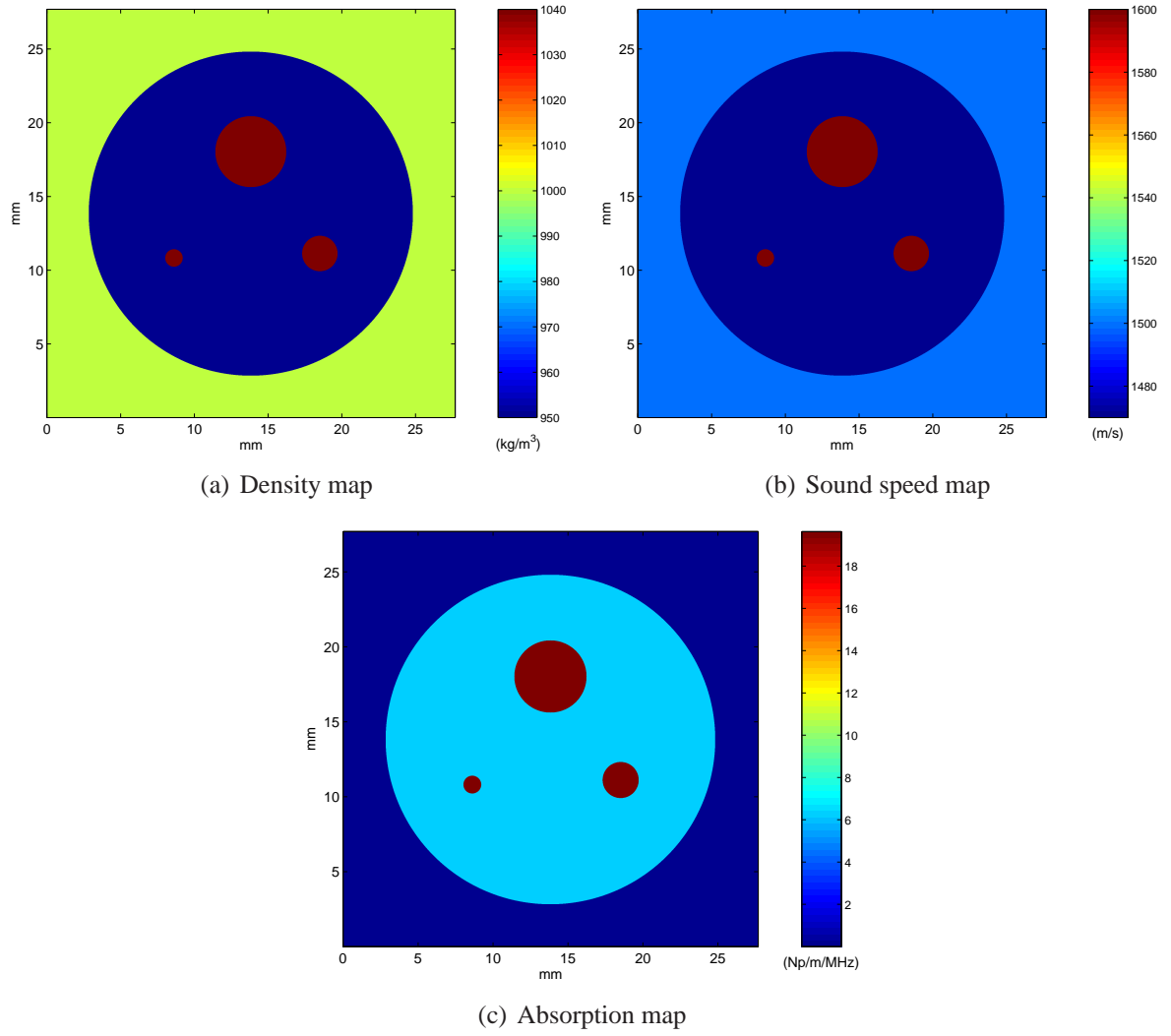


Figure 1: Cylindrical academic computer phantom.

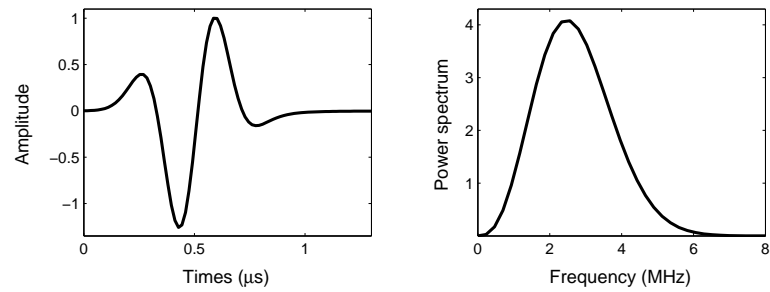


Figure 2: 2.5 MHz cylindrical wave used in the FEM simulations in time and in frequency.

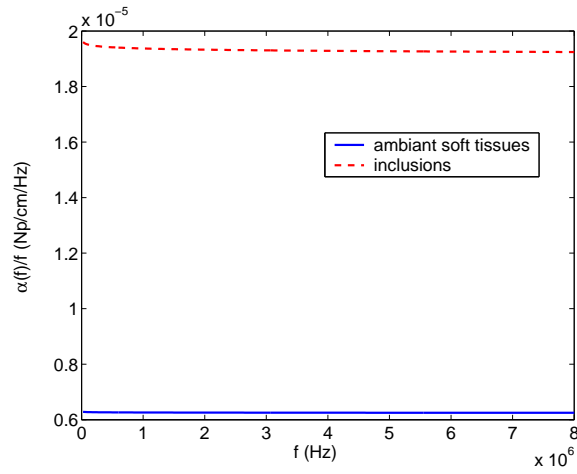


Figure 3: $\frac{\alpha(f)}{f}$ in function of f .

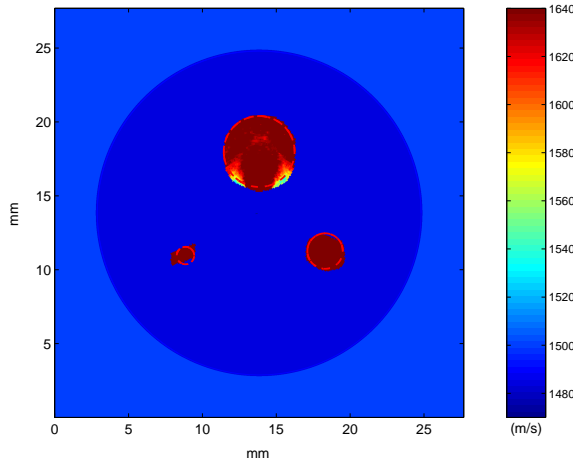


Figure 4: Reconstruction of the sound speed via the layer stripping technique.

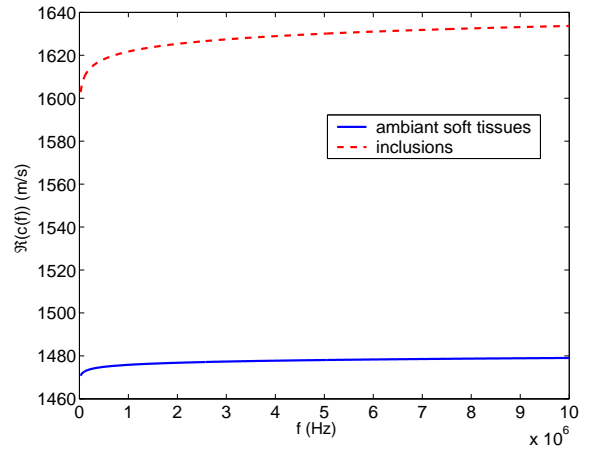


Figure 5: Evolution of the sound speed versus f .

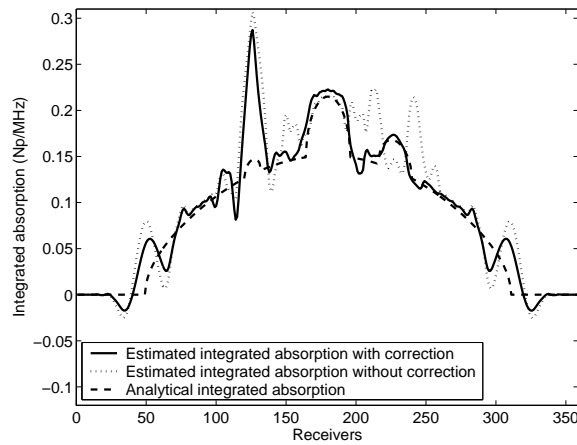


Figure 6: Projection data for one transmitter ($x=0.65$ mm, $y=13.85$ mm) using log spectra difference method with and without correction of the scattering effects.

errors were mainly due to the poor delimitation of the smallest inclusion in the sound speed map reconstruction (Fig. 4): figure 10 shows the tomographic reconstruction obtained when the correction was performed with a sound speed map drawn up with real size objects and the average sound speeds obtained via the layer stripping method (ambient soft tissues 1480 m/s and inclusions 1634 m/s). This greatly improved the absorption estimate of the smallest inclusions. The weakest point of this method is therefore the fact that it is sensitive to the discrimination of the inclusions of the same order of size as the wavelength (resonance phenomenon).

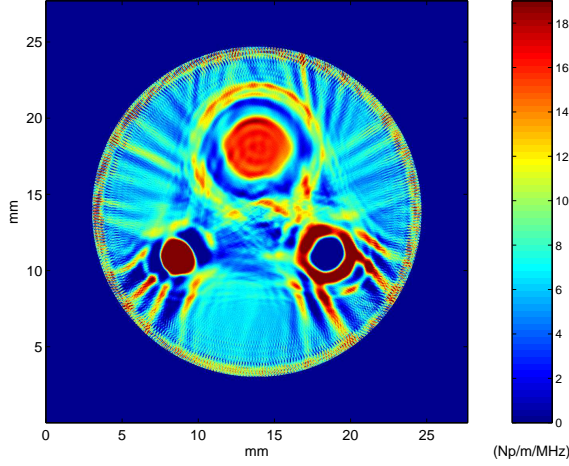


Figure 7: Reconstruction using classical log spectra difference technique.

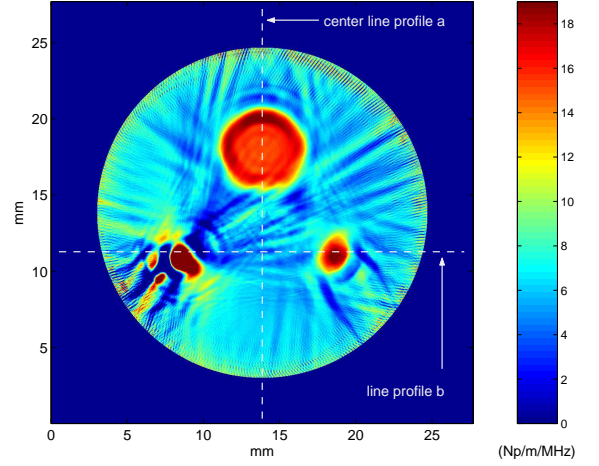
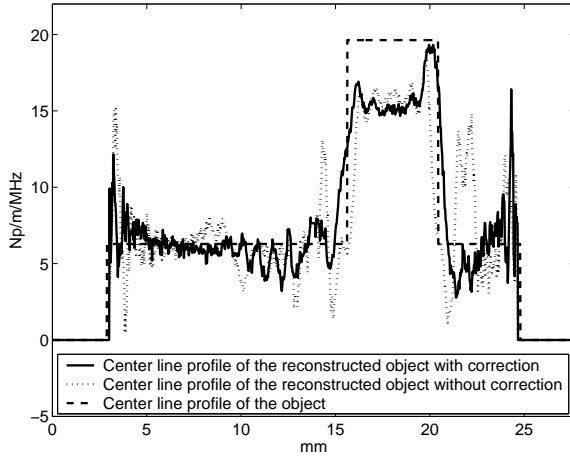
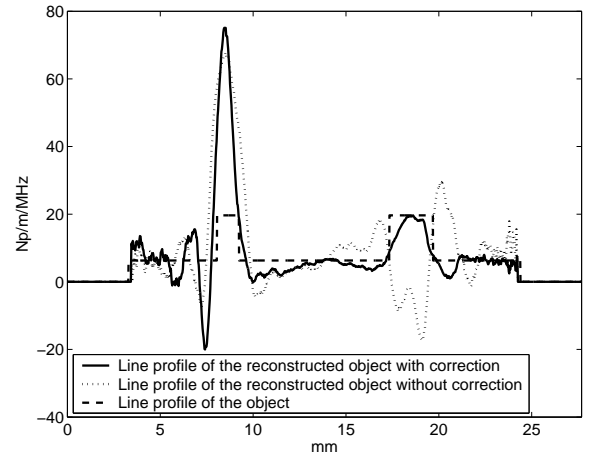


Figure 8: Reconstruction using log spectral difference technique with correction of the scattering effects.



(a)



(b)

Figure 9: Comparisons of the line profiles of the reconstructed object without (plotted line) and with (continuous line) correction of the scattering effects.

In conclusion, ultrasound scattering errors due to sound propagation occurring in inhomogeneous media blur the image and induce strong artefacts, especially if the size of the heterogeneities is of the same order as the wavelength. The reconstructions based on simulated data

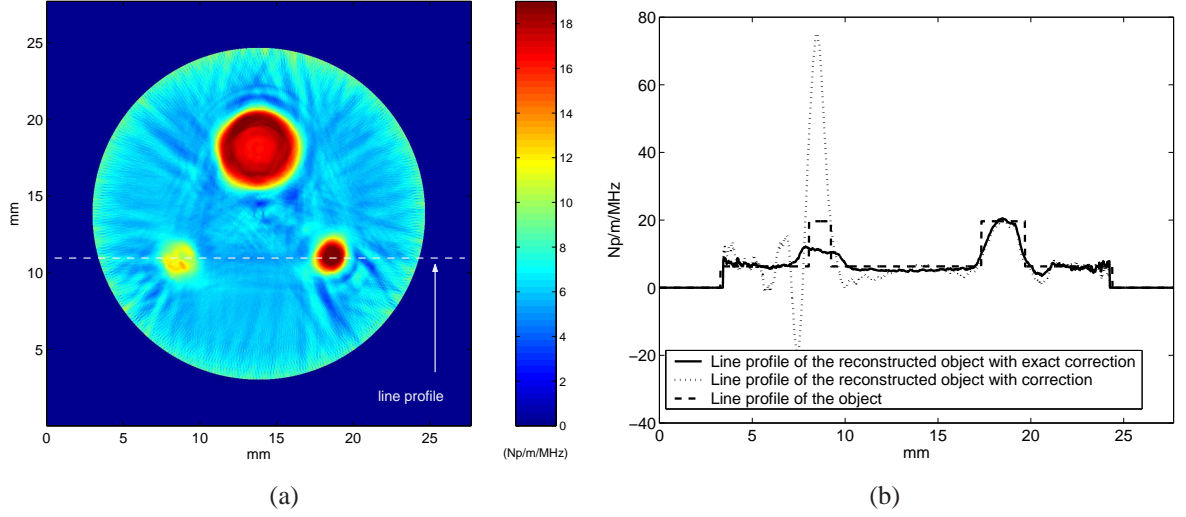


Figure 10: Reconstruction using log spectral difference technique with exact correction of the scattering effects (a) and line profile (b).

presented here show how applying scattering correction to the overall absorption estimates can improve the results obtained.

5 Conclusion

The artefacts observed in the tomographic reconstructions obtained using the classical log spectral difference technique have been mostly due to the fact that the scattering processes have been neglected. In order to overcome this problem, we have developed a method for estimating the scattering. Since this process results mainly from the propagation perturbations due to sound speed contrasts, a sound speed map was first reconstructed. This numerical model provided the input material for a time-domain finite element code simulating the wave propagation. This absorption free phantom mimics the tissues (viscous fluid) imaged except for the density and absorption characteristics: the density is taken a priori to be 1000 kg/m^3 , and the absorption is not taken into account. The impedance fluctuations in the object are therefore approximated in terms of the estimated sound speed contrast. This realistic numerical model can be used to predict the scattered field without any absorption interference, and this field constitutes our scattering distortion reference field in the log spectral difference absorption estimates. A tomographic procedure was used to reconstruct an absorption map of the tissue under investigation. Numerical simulations illustrate the results obtained at each step and comparisons show the improvement obtained in the absorption contrast estimates. These results show that even in the case of small speed variations ($1470 \text{ m/s} - 1600 \text{ m/s}$), the effects of the scattering are non-negligible and can greatly degrade the quality of absorption tomographic images.

In practical situations, the method used here to correct the experimental data may not be as efficient as with simulated signals. In this study, the simulated dissipative data to be corrected and the simulated non-dissipative data used for the correction were generated from two versions of the same propagation code. This situation will differ in experimental contexts, where the waves undergo all the propagation effects (3D, non linearity, etc). In addition, in practical situations, the active transducers are all distinct, non-punctual and have their own directivity in-

dex. Theoretically, this should not greatly affect the absorption measurements, but in practice, "calibration" and "spatial deconvolution" are known to be rather delicate processes.

In conclusion, the numerical computations presented here show that the scattering cannot be overlooked (even in soft tissues) when ultrasound absorption is evaluated using insertion techniques. The absorption tomographic reconstructions carried out here show the improvement that can be achieved using the method described. In the case of high contrast objects, current approaches which operate on phase estimates could be associated with this method to improve the velocity dispersion estimation.

Acknowledgements

This study was supported by Ville de Marseille, Région Provence-Alpes-Cote d'Azur, Conseil Général 13 and CNRS-LMA. The authors thank the Institute for Development and Resources in Intensive Scientific computing (IDRIS), where a some of the computations were performed. We are grateful to Chrysoula Tsogka (researcher at CNRS) for putting her propagation code at our disposal and Laurent Pruvost (EGIM) for his participation in the attenuation estimation procedure.

References

- [1] G. MCDANIEL, *Ultrasonic attenuation measurements on excised breast carcinoma at frequencies from 6 to 10 MHz*, in Ultrasonic Symp. Proc. IEEE. 77CH1264-ISU, pp. 234-236, 1977.
- [2] E. K. FRY, N. SANGHI, F. FRY, H. GALLAGER, Frequency dependent attenuation of malignant breast tumors studied by the fast Fourier transform technique, in *Ultrasound Tissue Characterization II*, Linzer M ed., pp. 85-92, NBS Special Publication 525 (US Government Printing Office, 1979).
- [3] R. KUC, *Clinical application of an ultrasound attenuation coefficient estimation technique for liver pathology characterization*, IEEE Trans. Biomed. Eng. BME-27, no. 6, pp. 312-319, 1980.
- [4] N. F. MAKLAD, J. OPHIR, V. BALSARA, *Attenuation of ultrasound in normal liver and diffuse liver disease in vivo*, Ultrasonic Imaging 6, pp. 117-125, 1984.
- [5] L. LANDINI, R. SARNELLI, F. SQUANTINI, *Frequency-dependent attenuation in breast tissue characterization*, Ultrasound Med. Biol. 11, pp. 599-603, 1985.
- [6] S. W. FLAX, N. J. PELC, G. H. GLOVER, F. D. GUTMANN, M. MCLACHLAN, *Spectral characterization and attenuation measurements in ultrasound*, Ultrasonic Imaging 5, pp. 95-116, 1983.
- [7] I. CLAEISSON, G. SALOMONSSON, *Estimation of varying ultrasonic attenuation*, Ultrasound Med. Biol. 11, pp. 131-145, 1985.

- [8] P. HE, J. F. GREENLEAF, *Application of stochastic analysis to ultrasonic echoes - Estimation of attenuation and tissue heterogeneity from peaks of echo envelope*, J. Acoust. Soc. Am. 79, pp. 526-534, 1986.
- [9] H. S. JIANG, T. K. SONG, S. B. PARK, *Ultrasound attenuation estimation in soft tissue using the entropy difference of pulsed echoes between two adjacent envelope segments*, Ultrasonic Imaging 10, pp. 248-264, 1988.
- [10] R. KUC, M. SCHWARTZ, *Estimating the acoustic attenuation coefficient slope for liver from reflected ultrasound signals*, IEEE Trans. Sonics Ultrason. SU-26, pp. 353-362, 1979.
- [11] C. R. MEYER, *An iterative, parametric spectral estimation technique for high-resolution pulse-echo ultrasound*, IEEE Trans. Biomed. Eng. BME-26, pp. 207-212, 1979.
- [12] K. A. DINES, A. C. KAK, *Ultrasonic attenuation tomography of soft tissues*, Ultrasonic Imaging 1, pp. 16-33, 1979.
- [13] P. A. NARAYANA, J. OPHIR, *Spectral shifts of ultrasonic propagation: A study of theoretical and experimental models*, Ultrasonic Imaging 5, pp. 22-29, 1983.
- [14] M. FINK, F. HOTTIER, J. F. CARDOSO, *Ultrasonic signal processing for in vivo attenuation measurement: short time fourier analysis*, Ultrasonic Imaging 5, pp. 117-135, 1983.
- [15] J. OPHIR, T. H. SHAWKER, N. F. MAKLAD, J. G. MILLER, S. W. FLAX, P. A. NARAYANA, J. P. JONES, *Attenuation estimation in reflection: progress and prospects*, Ultrasonic Imaging 6, pp. 349-395, 1984.
- [16] K. M. PAN, C. N. LIU, *Tomographic reconstruction of ultrasonic attenuation with correction for refractive errors*, IBM J. Res. Develop. 25, no. 1, pp. 71-82, 1981.
- [17] M. J. CLOOSTERMANS, J. M. THIJSEN, *A beam corrected estimation of the frequency dependent attenuation of biological tissues from backscattered ultrasound*, Ultrasonic Imaging 5, pp. 136-147, 1983.
- [18] M. INSANA, J. ZAGZEBSKI, E. MADSEN, *Improvements in the spectral difference method for measuring ultrasonic attenuation*, Ultrasonic Imaging 5, pp. 331-345, 1983.
- [19] M. O'DONNELL, *Effects of diffraction on measurements of the frequency dependent ultrasonic attenuation*, IEEE Trans. Biom. Engin. BME-30, pp. 320-326, 1983.
- [20] P. LAUGIER, G. BERGER, M. FINK, J. PERRIN, *Diffraction correction for focused transducers in attenuation measurements in vivo*, Ultrasonic Imaging 9, pp. 258-259, 1987.
- [21] W. XU, J. K. KAUFMAN, *Diffraction correction methods for insertion ultrasound attenuation estimation*, IEEE Trans. Biom. Eng. 40, no. 6, pp. 563-570, 1993.
- [22] C. M. SEHGAL, J. F. GREENLEAF, *Scattering of ultrasound by tissues*, Ultrasonic Imaging 6, pp. 60-80, 1984.
- [23] P. LAUGIER, G. BERGER, M. FINK, J. PERRIN, *Specular reflector noise: effect and correction for in vivo attenuation estimation*, Ultrasonic Imaging 7, pp. 277-292, 1985.

- [24] C. L. MORFEY, *Dictionary of acoustics*, Academic Press, pp. 110, 2001.
- [25] J. F. GREENLEAF, S. A. JOHNSON, S. L. LEE, G. T. HERMAN, E. H. WOOD, *Algebraic reconstruction of spatial distributions of acoustic absorption within tissue from their two dimensional acoustic projections*, in *Acoustical Holography 5*, Plenum Press, New York, pp. 591-603, 1974.
- [26] S. A. Johnson, J. F. Greenleaf, W. F. Samayoa, F. A. Duck, J. D. Sjosstrand, *Reconstruction of three-dimensional velocity fields and others parameters by acoustic ray tracing*, in *Proc. 1975 Ultrasonic Symposium*, pp. 46-51, 1975.
- [27] S. J. NORTON, M. LINZER, *Correcting for ray refraction in velocity and attenuation tomography: a perturbation approach*, *Ultrasonic imaging* 4, pp. 201-233, 1982.
- [28] C. SEHGAL, J. F. GREENLEAF, *Ultrasonic absorption and dispersion in biological media: a postulated model*, *J. Acoust. Soc. Am.* 72, no. 6, pp. 1711-1718, 1982.
- [29] J. P. GROBY, C. TSOGKA, *A time domain method for modeling wave propagation phenomena in viscoacoustic media*, in *Proc. 6th Inter. Conf. on Maths. and Num. Aspects of Wave Propag.*, pp. 911-915, 2003.
- [30] J. P. GROBY, C. TSOGKA, *A time domain method for modeling viscoacoustic wave propagation*, *J. of Comput. Acoustics*, in press, 2005.
- [31] R. FERRIERE, S. MENSAH, *Weakly Inhomogeneous Media Tomography*, *Ultrasonic Imaging* 25, pp. 122-133, 2003.
- [32] S. MENSAH, R. FERRIERE, *Diffraction tomography: a geometrical distortion free procedure*, *Ultrasonics* 42, pp. 677-682, 2004.
- [33] A. C. KAK, M. SLANEY, *Principles of computerized tomographic imaging*, IEEE Press, pp. 77-86, 1988.